Subliming Ice Surfaces: Freeze-Etch Electron Microscopy

Abstract. *Vacuum sublimation of oriented single crystals of ice at temperatures from −110 to −60 degrees Celsius was studied by electron microscopy with the freeze-etch technique. Sublimation etches the ice surface to produce pits and asperities and above −85 degrees Celsius causes extreme surface roughening. The etch pits are ascribed to surface dislocations, and the extreme roughening is ascribed to the departure from unity of the vaporization coefficient. The asperities could not be attributed to impurities; they may be related to the whiskers that others have observed at higher temperatures.*

The freeze-etch technique (FET) has provided a very useful means of studying biological fine structure (*1, 2*). It should also prove useful to the physical scientist interested in the surface morphology of solids that sublime below room temperature. The FET depends on electron microscopic examination of the replica of an etched fracture plane in a frozen specimen. With reference to biological materials, "etched" means that the three-dimensional relief of a fracture through the frozen specimen is enhanced by subliming water molecules away from nonvolatile constituents such as proteins, lipids, or carbohydrates. Very little is known about the morphological changes that occur on ice surfaces during sublimation at low temperatures under high vacuum (*3*).

In the first paper describing the construction and use of a freeze-etch device, Moor *et al.* (*1*) noted asperities with diameters of 10 to 30 nm, which they called "warts," on the etched surface of ice. Although numerous investigations have subsequently utilized the FET to investigate the structure of biological specimens in an aqueous milieu, the presence of these warts on the etched ice surface has either been ignored or ascribed to some undefined contaminant. Instead, attention has focused on numerous particles seen in many cellular membranes (*2, 4*). These biological particles can usually be distinguished from the ice warts because the biological particles are usually smaller in diameter, more limited in distribution, and occur in freshly fractured, unetched preparations (the ice warts appear only after sublimation). However, further differentiation of the two structures would be important both for the interpretation of biological structure in freeze-etch replicas and for the understanding of the ice sublimation mechanism. We have therefore correlated structural and kinetic approaches in this study of ice crystal sublimation.

We grew ice from distilled water by the method of Jona and Scherrer (*5*) (Fig. 1a) and mounted a single ice crystal (Fig. 1b) so that basal-face (*c*-face) samples had the *c* axis vertical; "prism-face" samples had the *c* axis horizontal. Note that, in the prism-face samples, an *a* axis was not necessarily vertical, and thus the true prism-face orientation was not fully determined. The orientation of the various axes and faces for ice is indicated in Fig. 1e.

Multiple knife passes fractured the mounted samples (Fig. 1, c and d) to produce a macroscopically flat surface. Immediately after the last pass, the knife was positioned about 1 mm above the surface to act as a cold trap and to minimize the chance for condensation of any vacuum contaminant on the sample surface (*6*). After the sample had been etched for the chosen period, the knife was moved away and a replica was immediately produced by simultaneous vapor deposition of carbon and platinum (*1*). The sample was removed from the freeze-etch machine and was thawed, and the replica was placed on a grid for examination in the electron microscope.

The maximum rate at which a material could sublime can be calculated

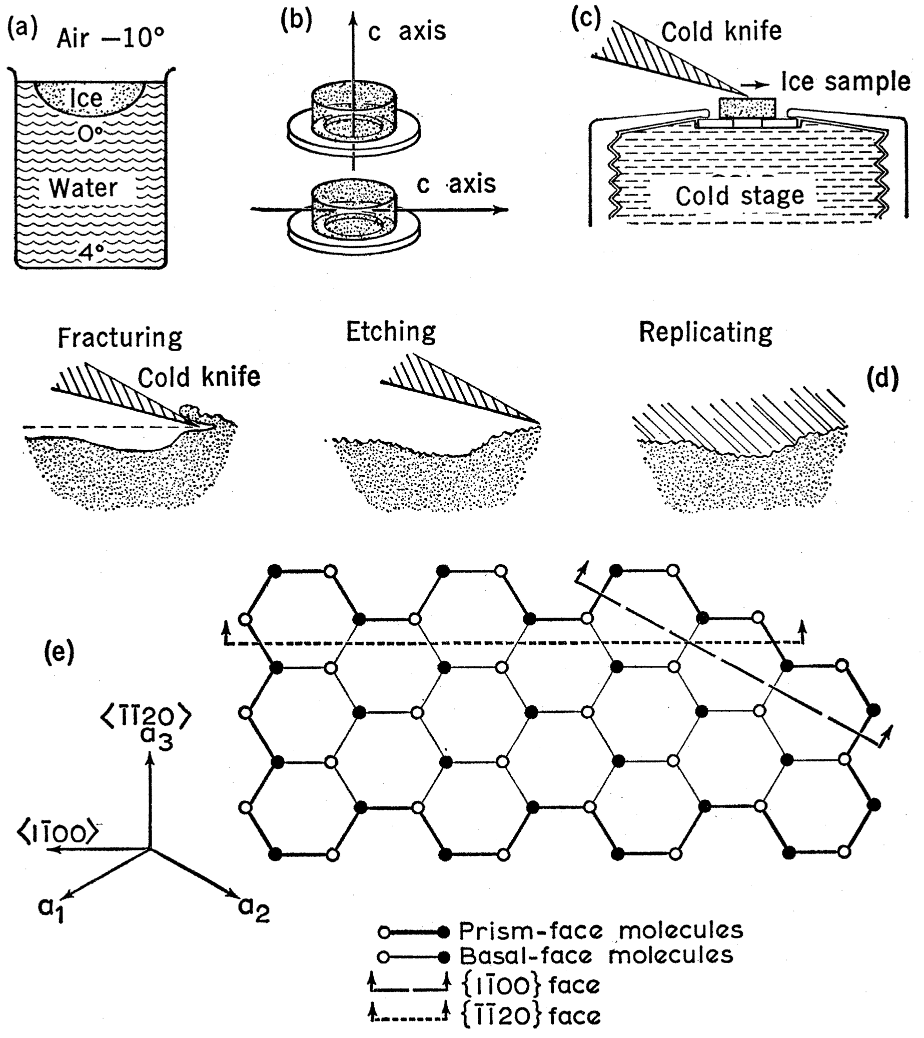

Fig. 1. Experimental approach. (a) Ice is crystallized slowly from the melt in a 600-ml beaker. (b) Polarizing optics are used to select a single-crystal region from which small disks are cut. The disks are frozen to 5-mm washers, and the orientation is rechecked. (c) The mounted sample is clamped on a cold stage (temperature adjustable to ± 0.1°C), and (d) the sample is fractured, etched, and replicated. The knife is maintained at −196°C. (e) Basal face (*c* face) of hexagonal ice. Open circles are 0.09 nm above filled circles. The edge-on views of two prism faces (one *a* $\{\bar{1}\bar{1}20\}$ face and one $\{\bar{1}100\}$ face) are indicated. Both have shallow trenches (0.238 and 0.138 nm, respectively) running parallel to the *c* axis.

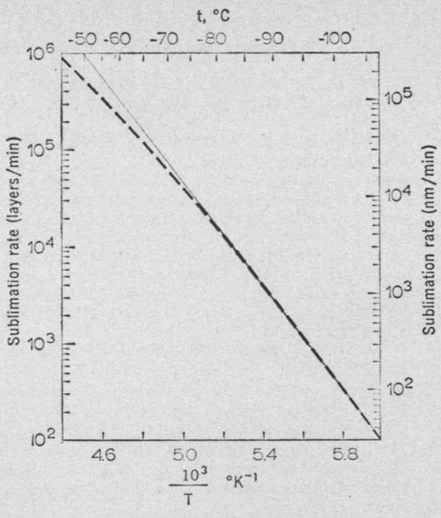

Fig. 2. Ice vaporization rate versus temperature. Solid line, theoretical rate; dashed line, measured rate.

from its vapor pressure. The actual rate cannot be calculated but must be measured under vacuum conditions (to assure negligible gas-phase collisions of the evaporated molecules). Such studies have been made on single crystals of ice with microbalance techniques (*7*). Figure 2 shows both the theoretical maximum and the observed rates as a function of temperature. The ratio of these two rates is called the vaporization coefficient: $\alpha_v(T) \equiv$ observed rate divided by theoretical rate. No orientation dependence of the rate has been found, but, at temperatures above about −85°C, the observed rate begins to fall below the theoretical rate (α_v begins to fall below unity). This phenomenon implies that for the higher temperatures there is some rate-limiting step prior to desorption in the evaporation process. It has been observed (*8*) that, in materials with $\alpha_v < 1$, sublimation may produce surface roughening. Surface roughening increases the total surface area and gives a vaporization rate between the rate observed from a hypothetical flat surface with the true α_v and the rate from a flat surface with $\alpha_v = 1$.

Electron micrographs of ice surface replicas obtained by the FET are shown in Fig. 3. The variables of interest are the orientation, the temperature, and the duration of sublimation. Figure 3a shows a crystal that was cleaved and then replicated before any significant etching had occurred. The largest part of the surface is smooth and rounded out by conchoidal fracture. This appearance is quite general; it does not depend on orientation or sample temperature. The various fracture modes observed are believed to be due to local variations in the rate and direction of fracture propagation.

In Fig. 3b, a basal-face sample is shown; Fig. 3c shows a prism-face sample. Both samples were etched 1 minute at −100°C, which corresponds to a loss of 120 nm. The basal face exhibits round, flat-bottomed etch pits about 1 μm in diameter (*9*). One etch pit is shown in Fig. 3b. The entire surface is covered with asperities, which are relatively featureless and which have a maximum size of about 30 nm. Their average density on any sample is about 200 per square micrometer, but this density varies within a factor of 2 from place to place within a sample. Within etch pits the asperities are smaller. The prism-face samples exhibit two kinds of etch pits, apparently on different crystallographic faces. The round kind are indistinguishable from the pits on basal-face samples, but the rectangular pits are obviously different. Stair-step ledges extend up their walls, where the asperities appear elongate. The pit edges are parallel and perpendicular to the *c* axis, and the flat pit bottoms are free from asperities.

In a series of samples etched at different temperatures for times calculated to produce equivalent etching, those at −110°C looked like those etched at −100°C. However, sublimation at higher temperatures did change surface morphology. In prism-face samples etched at −90°C (Fig. 3d), the sharp edges of etch pits are not so well developed

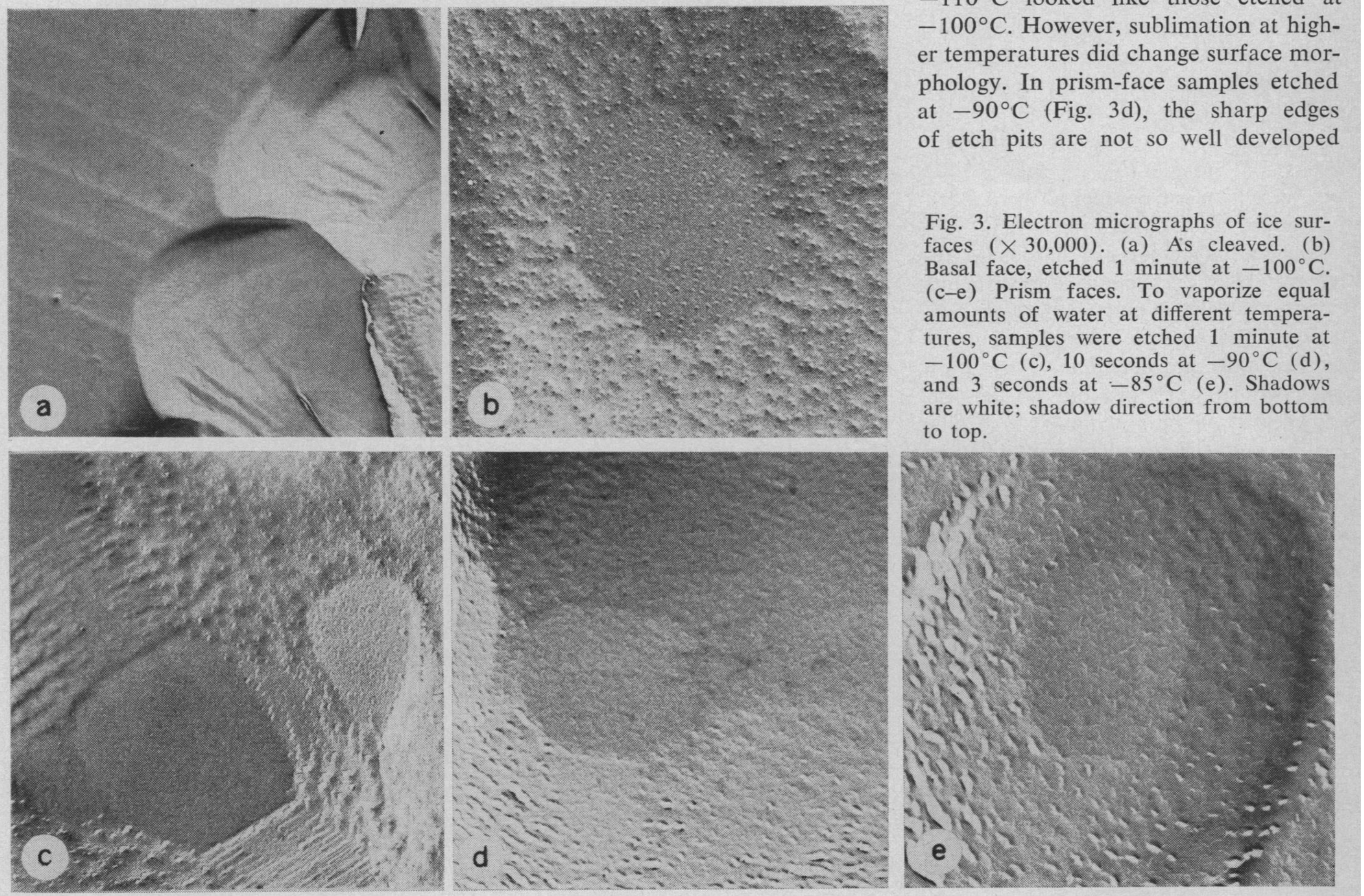

Fig. 3. Electron micrographs of ice surfaces (× 30,000). (a) As cleaved. (b) Basal face, etched 1 minute at −100°C. (c–e) Prism faces. To vaporize equal amounts of water at different temperatures, samples were etched 1 minute at −100°C (c), 10 seconds at −90°C (d), and 3 seconds at −85°C (e). Shadows are white; shadow direction from bottom to top.

and the asperity density is about one-third that observed at $-100°C$. At $-85°C$ (Fig. 3e), all etch pits are round and the asperities, which appear as warts at $-100°C$, now appear as holes in the replica. At higher temperatures ($-75°C$, $-60°C$), these holes become progressively larger and the surface becomes so extremely rough that we could not produce a continuous replica with our technique.

In another series (not shown) in which longer times of sublimation were used, the characteristic etch pits defined by temperature and orientation grew larger and shallower until, after about 10 μm of ice had etched away, they merged and were no longer evident. Long periods of etching appeared to cause a slight increase in the average number and size of the asperities, but never by a factor of more than 2.

Since the etch pits appear in large numbers at the edges of the fracture conchoids and are relatively rare at their centers, it seems likely that surface dislocations, introduced by the cleaving, initiate the pits. The strain fields do not penetrate far below the surface, and soon a relatively stable, low-index face develops and grows (*10*).

Apparently the faces $\{0001\}$ (*c* face), $\{\bar{1}\bar{1}20\}$ (*a* face), and $\{1\bar{1}00\}$ are slightly more stable kinetically than other (random) faces. On prism-face samples at all temperatures, very small amounts of etching are sufficient to reveal the direction of the ***c*** axis, owing to the tendency of the $\{\bar{1}\bar{1}20\}$ or the $\{1\bar{1}00\}$ planes (which are parallel to the *c* axis), or both, to develop as facets (*11*).

Surface asperities are harder to interpret. Neither vacuum contaminants nor the cleavage and replicating procedures can explain their development because they are completely absent on unetched surfaces and on the flat-bottomed part of the rectangular etch pits. Furthermore, their appearance changes over the 15° interval from $-100°$ to $-85°C$. It is also highly improbable that the asperities are due to dislocations, as their density (200 per square micrometer) is three to four orders of magnitude higher than the highest dislocation densities observed in nonmetals.

We can explain the asperities and their temperature-dependent appearance on the basis of the following assumptions: (i) The ice contains domains whose effective vaporization coefficient is lowered to a value $\alpha_v' < \alpha_v$. (ii) The domains sublime or blow away (*12*) when exposed at the ice surface. (iii) The temperature dependence of α_v' is not necessarily the same as that of α_v. The absence of asperities on the rectangular etch pit bottoms would imply that for this crystal face $\alpha_v' = \alpha_v$ for temperatures less than $-90°C$.

Microbalance studies show that a variety of ionic impurities can lower the vaporization rate (*13*). Domains with lowered vaporization coefficients could be attributed to such impurities (*14*). We have examined replicas of ice samples deliberately doped with deuterium oxide (*15*) or ammonium fluoride [NH_4F does lower α_v (*13*)], rapidly frozen samples of high purity (resistivity, > 18 megohm cm) (*16*), and samples degassed and frozen under vacuum to minimize gaseous contaminants. None of these treatments altered the asperity density. It is therefore improbable that the asperities are produced by impurities.

At temperatures above $-55°C$, elongate whiskers have been observed on subliming ice surfaces (*17*). They have been attributed to surface migration and recondensation phenomena, but the underlying factors that can explain their origin are unknown. The asperities seen at the low temperatures that we investigated may be primitive forms of these whiskers. If so, the holes and extreme roughening in the replicas of ice vaporizing at temperatures above $-90°C$ could be the result of tall, thin asperities (whiskers), whose replica would be too delicate to survive melting of the sample and transfer of the replica to the electron microscope grid.

Our studies have shown that the subliming ice surface displays features that vary remarkably in appearance as a function of crystal orientation and temperature in the range $-100°$ to $-85°C$. We have also found that, for given conditions, the surface takes on a characteristic steady-state appearance by the time 100 nm of the ice have been removed; subsequent sublimation makes only slow changes in this appearance. These temperature-dependent topographical features of ice should be taken into account by those interested in the mechanism of sublimation or the interpretation of structure in hydrated, freeze-etched samples.

J. GORDON DAVY*
Department of Chemistry, University of California, Berkeley 94720
DANIEL BRANTON
Department of Botany,
University of California, Berkeley

References and Notes

1. H. Moor, K. Mühlethaler, H. Waldner, A. F. Wyssling, *J. Biophys. Biochem. Cytol.* **10**, 1 (1961).
2. H. Moor and K. Mühlethaler, *J. Cell Biol.* **17**, 609 (1963).
3. Previous photographic studies of the ice surface have been made at temperatures above —25°C, at or near 1 atmosphere pressure. See, for example, D. Kuroiwa and W. R. Hamilton, in *Ice and Snow*, W. D. Kingery, Ed. (M.I.T. Press, Cambridge, 1963), p. 34; R. Levi *et al., Phys. Status Solidi* **4**, 63 (1963); F. Truby, *J. Appl. Phys.* **26**, 1416 (1955); see also reference (*17*).
4. D. Branton, *Annu. Rev. Plant Physiol.* **20**, 209 (1969).
5. F. Jona and P. Scherrer, *Helv. Phys. Acta* **25**, 35 (1952). For a discussion in English, see R. Siksna, *Ark. Fysik* **11**, 495 (1957).
6. The background pressure of 2×10^{-6} torr corresponds to each surface molecule being visited twice a second by residual gas molecules.
7. J. G. Davy, in *Vacuum Microbalance Techniques,* A. W. Czanderna, Ed. (Plenum, New York, in press), vol. 8; ——— and G. A. Somorjai, in preparation.
8. G. A. Somorjai, in *Advances in High-Temperature Chemistry* (Academic Press, New York, 1968), vol. 11, chap. 5, p. 203.
9. Flat-bottomed etch pits have been reported for ice at high temperatures after chemical etching (see *3*), but etch pits are predominantly pyramidal under these conditions. We have observed no etch pits without flat bottoms.
10. The nature of dislocations in ice is at present not well determined. Drost-Hansen and coworkers suggest the existence of dislocation rings with a central strain core of radius 0.4 μm [A. L. Gentile and W. Drost-Hansen, *Naturwissenschaften* **43**, 274 (1956)]. Webb and Hayes found, with the use of x-ray diffraction topography, large regions in ice that appeared to be free from dislocations. They point out, however, that their technique would not detect dislocation rings with a radius less than 25 μm [W. W. Webb and C. E. Hayes, *Phil. Mag.* **16**, 909 (1967)]. Ice dislocations are also discussed by A. Fukuda and A. Higashi [*Jap. J. Appl. Phys.* **8**, 993 (1969)] and by authors in reference (*3*).
11. For a good discussion of thermal faceting on other materials, see A. J. W. Moore, in *Metal Surfaces,* W. D. Robertson and N. A. Gjostein, Eds. (American Society for Metals, Novelty, Ohio, 1963), p. 155.
12. R. I. N. Greaves, in *Biological Applications of Freezing and Drying*, R. J. C. Harris, Ed. (Academic Press, New York, 1954), p. 125; D. W. Deamer and D. Branton, *Science* **158**, 655 (1967).
13. J. G. Davy, thesis, University of California, Berkeley (1970); Lawrence Radiation Laboratory Report UCRL No. 19133 (1970).
14. The impurity concentration required to account for the asperities can be calculated as follows: Let a be the distance between neighboring water molecules in ice (about 0.3 nm). The number of water molecules in a single lattice plane is about $10^7/\mu m^2$. The observed number of asperities per square micrometer is about 200. If spherical domains with maximum radius r are assumed, asperities would be due to impurities in $2r/a$ layers. Maximum asperity radius is about 15 nm. The impurity concentration is therefore $(200/10^7) \div [(2 \times 15)/0.3] = 0.2$ parts per million.
15. Two percent D_2O in H_2O. Pure etched D_2O ice looked like H_2O ice.
16. Even if we include the free H^+ and OH^- ions as impurities, the total ionic impurity concentration of water with this resistivity is less than 0.01 part per million. Actually, the H^+ and OH^- concentration in ice would be lower than in the melt.
17. S. M. de Micheli and A. R. Licenblat, *J. Atmos. Sci.* **24**, 312 (1967); L. V. Lukov *et al., Inzh. Fiz. Zh.* **15**, 782 (1968); J. D. Cross, *Science* **164**, 174 (1969).
18. We thank Susan Whytock for expert technical assistance. Research supported by the Atomic Energy Commission.

* Present address: RCA Laboratories, Princeton, N.J. 08540.

20 January 1970; revised 8 April 1970